

Cold Reactions of Alkali-Metal and Water Clusters inside Helium Nanodroplets

S. Müller,¹ S. Krapf,² Th. Koslowski,² M. Mudrich,^{1,*} and F. Stienkemeier¹

¹Physikalisches Institut, Universität Freiburg, 79104 Freiburg, Germany

²Institut für Physikalische Chemie, Universität Freiburg, 79104 Freiburg, Germany

(Received 28 October 2008; published 8 May 2009)

The reaction of alkali-metal (Na, Cs) clusters with water clusters embedded in helium nanodroplets is studied using femtosecond photoionization as well as electron-impact ionization. Unlike Na clusters, Cs clusters are found to completely react with water in spite of the ultracold helium droplet environment. Mass spectra of the $\text{Cs}_n + (\text{H}_2\text{O})_m$ reaction products are interpreted in terms of stability with respect to fragmentation using high-level molecular structure calculations.

DOI: 10.1103/PhysRevLett.102.183401

PACS numbers: 36.40.Jn, 34.50.Lf, 36.40.Qv, 82.33.Fg

Chemical reactivity at very low temperatures is a topic of increasing interest both for theory and for experiment [1–4]. Cold reactive ion-molecule collisions have recently been reported [4], and experiments aiming at studying cold reactive neutral molecule-molecule collisions using Stark-decelerated molecular beams are in preparation [2,5].

Helium (He) nanodroplets are particularly well suited as a nearly ideal cryogenic matrix for studying reactions at sub-Kelvin temperatures [3,6]. The high mobility of dopant atoms and molecules inside the superfluid droplets allows one to bring together atoms or molecules of rather different nature [6]. While the He droplet environment has only a very weak influence on the rovibronic structure of embedded ground state molecules, their internal degrees of freedom are efficiently cooled to the droplet temperature (0.4 K) by evaporation of He atoms [6]. This may lead to the aggregation of weakly bound complexes and to the stabilization of reaction intermediates in local minima of the potential energy surface.

So far, the only chemical reaction involving neutral heterogeneous reactant molecules inside He nanodroplets is $\text{Ba} + \text{N}_2\text{O} \rightarrow \text{BaO} + \text{N}_2$, which was characterized by chemiluminescence spectroscopy [7]. Recently, some efforts for exploring chemical reactions in He droplets have been made, e.g., on the reaction $\text{F} + \text{CH}_4$ [8]. However, no reactive process was found indicating that at the low temperature of the He droplet environment even small energy barriers may impede chemical reactions. Beside the reaction of neutrals, a rich ion-molecule chemistry inside ionized He droplets has been reported [6]. For example, secondary reactions of N_2^+ , D_2^+ , and CH_4^+ fragment ions created by electron-impact ionization (EII) of the He have been identified, thus evoking the term “flying nanocryoreactors” [9].

The showcase reaction $\text{Na} + \text{H}_2\text{O}$ has been studied in great detail at higher temperatures to solve the long-standing puzzle [10–15]: While alkali metals are well known to react with water in a violent exothermic reaction at the macroscopic scale, single Na atoms colliding with water molecules or even with clusters do not react. Only

when combining Na clusters with H_2O clusters were chemical reactions found to take place, and products of oxidative hydrolysis $\text{Na}(\text{NaOH})_n^+$ appeared in the mass spectra [14,15]. Both experimental and theoretical results point at a complex elementary reaction involving three Na atoms and six H_2O molecules [13,15]. In this Letter, we report on the chemical reaction of alkali-metal (Na, Cs) clusters with H_2O clusters inside He nanodroplets. We have done similar studies using K and Rb; these results nicely go along with the interpretations given below and will be published elsewhere.

Our experiment combines a beam of He nanodroplets, consecutively doped with on average 20 H_2O molecules and 10 alkali-metal atoms, with femtosecond photoionization (PI). The experimental setup is described in detail elsewhere [16]. In short, ultrapure He gas is expanded at high pressure (60 bar) out of a cryogenic nozzle (diameter 10 μm) into high vacuum. At the nozzle temperature of 13 K, the average droplet size amounts to about 20 000 atoms. In order to obtain a realistic picture of the compounds produced in the reaction, two complementary ionization schemes are employed—nonresonant multiphoton PI using laser pulses of 150 fs duration at 860 nm [755 nm] for the Cs [Na] experiments and EII at 30 eV electron energy.

The resulting PI mass spectrum of He droplets simultaneously doped with Na_n and $(\text{H}_2\text{O})_m$ is displayed in Fig. 1. It is clearly dominated by small clusters Na_{1-3} carrying up to 8 water molecules reflecting weakly bound van der Waals complexes (upper 3 panels) [17]. The only masses originating from the reaction with H_2O are low-abundant Na hydroxide compounds $\text{Na}(\text{NaOH})_n$, where the most prominent peak is $\text{Na}(\text{NaOH})_2$ (bottom panel). This finding is in line with cluster reactions being largely frozen out in the ultracold droplet environment, except for a small fraction that has not completely thermalized to 0.4 K before initiating the reaction.

However, a totally different picture presents itself when Cs clusters are combined with H_2O clusters inside He droplets. The PI mass spectrum, shown in Fig. 2(a), fea-

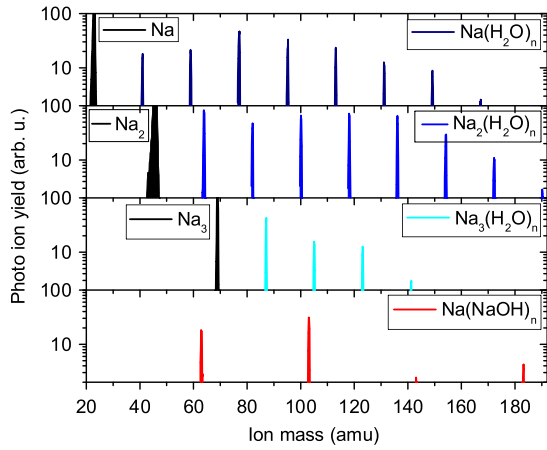


FIG. 1 (color online). PI mass spectrum of mixed sodium (Na)-water (H_2O) clusters in He nanodroplets. For the sake of clarity, the dominant progressions $\text{Na}(\text{H}_2\text{O})_n$, $\text{Na}_2(\text{H}_2\text{O})_n$, $\text{Na}_3(\text{H}_2\text{O})_n$, and $\text{Na}(\text{NaOH})_n$ are represented separately.

tures a number of additional peaks aside from the pure Cs_n masses, which follow a strikingly regular pattern: Roughly speaking, every Cs_n cluster mass peak is augmented by $n - 1$ satellites with additional masses of about 1 to $n - 1$ water molecules. Except for the Cs_2 satellite, the last peak of each series, corresponding to $\text{Cs}(\text{CsOH})_n$, shows extra-

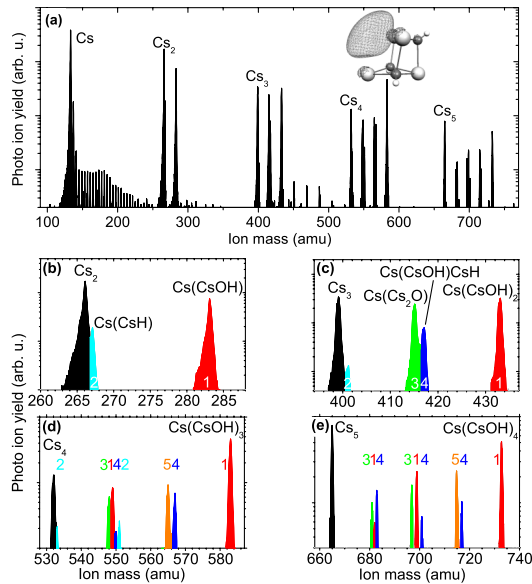


FIG. 2 (color online). (a) Photoionization mass spectrum of mixed cesium-water clusters in He nanodroplets. The inset illustrates the molecular structure of the prominent compound $\text{Cs}(\text{CsOH})_3^+$ (see text). (b)–(e) Detailed views of the mass spectrum in the mass ranges of Cs_{2-5} and associated reaction products. Colored indices 1–6 label different types of product compounds: (1) hydroxides $\text{Cs}_n(\text{CsOH})_m$, (2) hydrides $\text{Cs}_n(\text{CsH})_m$, (3) oxides $\text{Cs}_n(\text{Cs}_2\text{O})_m$, (4) mixed compounds containing hydroxide and hydride $\text{Cs}_n(\text{CsOH})_m\text{CsH}$, and (5) hydroxide and oxide $\text{Cs}_n(\text{CsOH})_m\text{Cs}_2\text{O}$.

ordinarily high abundance, in the case of $\text{Cs}(\text{CsOH})_3$ even exceeding the one of the corresponding neat cluster Cs_4 . However, no van der Waals-bound complexes $\text{Cs}_n(\text{H}_2\text{O})_m$ with $m \geq n$ are observed under any conditions, in contrast to the $\text{Na}_n + (\text{H}_2\text{O})_m$ system.

Upon closer inspection, the satellite peaks reveal a more complex composition reflecting different reaction products [Figs. 2(b)–2(e)]. These compounds are found to follow odd-even alternations in terms of the number of Cs atoms involved. For example, Cs_nO and Cs_nOH_2 are most abundant for odd n , whereas Cs_nH and $\text{Cs}_n(\text{OH})_{n-1}$ mass peaks are more pronounced for even n . This suggests the notation used in the caption of Fig. 2 which is in accordance with valencies of the atomic and molecular constituents.

The surprising result of this experiment is that small clusters Cs_n actually react very efficiently with water inside He nanodroplets, despite the low temperature environment. This implies nearly vanishing activation energy for cluster reactions involving Cs, in contrast to the findings for the reaction of Na and Na_2 with water [13,14]. From the reactivity of bulk alkali metals with water, it is well known, though, that Cs has a much lower activation energy than Na. Besides, a decrease of the reaction barrier with increasing size of the alkali-metal cluster is expected [12,14,15]. In He droplets, the reaction might be facilitated by the alkali clusters being partly or fully spin-polarized [18]. However, under the conditions of the present experiment—when doping much larger droplets with many alkali-metal atoms—these clusters are formed predominantly in conventional low-spin states [19]. Hence, in terms of spin configurations, the reaction with water does not differ from other experiments. Strong reactivity of Cs_n with $(\text{H}_2\text{O})_m$ in He droplets may also seem unexpected considering the fact that Cs atoms, molecules, and presumably clusters are located in surface states whereas water molecules are immersed inside the droplets. However, it is known from previous experiments on alkali-metal and alkaline-earth-metal atoms codoped with solvated molecules HCN and N_2O , respectively, that different initial positions in or on the droplets do not hamper their reaction due to the action of long-range attractive forces [7,17]. Even the locally enhanced He density that surrounds embedded ions has not appeared to suppress their reactivity [3,9].

The possibility of reactions of the ionized clusters taking place after PI instead of occurring spontaneously among the neutrals can be excluded for the following reasons. The solvation of the valence electron of an alkali-metal atom in water was found to be crucial for initiating the reaction due to its acting as a catalyst [13,15]. In contrast, alkali-metal ions do not react with water. Ionized alkali-metal clusters may produce solvated electron(s), which, however, seems not very likely given the limited size of the water clusters [20]. Besides, in earlier experiments on alkali-metal-doped water clusters, no indication for the initiation of reactions

by nanosecond PI has ever been reported [10,11,14,15]. Experimental evidence for reactions to proceed prior to PI is obtained from the comparison of EII and PI mass spectra recorded under identical conditions. While femtosecond PI acts on the alkali-metal atoms and clusters due to their low ionization potentials ($\sim 2.7\text{--}5$ eV), it is completely inefficient for pure water clusters. In contrast, EII proceeds in a two-step process mediated by the He atoms [6]. Thus, $(\text{H}_2\text{O})_m$ clusters, which are immersed into the droplets, are more easily ionized by EII than the neat alkali-metal clusters, which stay bound to the droplet surface. Despite the different ionization mechanisms, mass spectra obtained with EII and PI show a great resemblance, as illustrated in Fig. 3. EII mass spectra of the lighter alkali-metal atoms reacting with water are more congested due to the presence of neat water clusters, but the number of water attachments as compared to reaction products is again comparable using the two ionization schemes. We conclude that these spectra actually reproduce the abundance distributions of ionized compounds and that reactions take place among neutral precursor clusters before ionization. Slight differences in the mass spectra can be attributed to varying degrees of fragmentation of the individual compound clusters due to the differing excess energies deposited in the clusters. This conclusion is backed by the fact that femtosecond PI spectra in the laser wave length range $\lambda = 700\text{--}950$ nm recorded at the masses of individual neat clusters Cs_n and corresponding compounds show no correlation. For example, Cs_{2-5} PI spectra feature broad maxima around $\lambda = 767, 740, 890,$ and 910 nm, respectively, in contrast to peaks found at $\lambda = 725, 723,$ and 706 nm in the PI spectra of $\text{Cs}(\text{CsOH})_{1-3}$, respectively, in addition to a common broad feature around $\lambda = 795$ nm on a high constant signal level ($\approx 50\%$). This demonstrates the fact that different neutral species are probed that must have formed prior to PI.

In order to interpret the observed abundance distributions of product masses, we have determined equilibrium structures, ionization potentials (IPs), and stabilities with

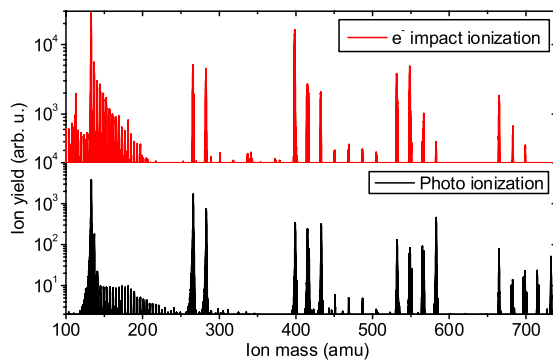


FIG. 3 (color online). Mass spectra of mixed cesium-water clusters in He nanodroplets, recorded using electron-impact ionization (upper trace) vs femtosecond photoionization at 860 nm (lower trace).

respect to fragmentation from high-level quantum chemical calculations for all observed compounds. Calculations are done with the GAUSSIAN 03 program package [21] using hybrid Hartree-Fock density functional theory with the 1997 hybrid exchange-correlation functional of Perdew, Burke, and Ernzerhof [22]. On Cs, a relativistic core potential [23] with the corresponding basis sets is used for single point calculations on previously optimized geometries; on H and on second row atoms the 6-311 + +G(3df, 3pd) basis is used. This method is found to reproduce the experimental atomization energies of Cs_2 , Cs_2O , CsOH , CsH , CsF , and CsCl with a mean deviation of ≤ 0.2 eV.

The theoretical results show that all detected compound masses feature low vertical IP < 3.3 eV and are thus amenable to efficient ionization by 2 or 3 photons from our femtosecond laser. It turns out that, while the likely reaction products (provided water is present in excess of Cs) $(\text{CsOH})_n$ require high energies $\Delta E > 3$ eV to fragment [Fig. 4(a), circles], the ionization products $(\text{CsOH})_n^+$ are quite unstable with respect to the most likely fragmentation channel, the loss of OH [Fig. 4(a), crosses]. This explains the lack of $(\text{CsOH})_n^+$ signals in both EII and PI mass spectra. In particular, for all clusters $(\text{CsOH})_n^+$ with $n \leq 4$, we find low fragmentation energies $\Delta E < 1$ eV that fall below the excess energies (difference between multiphoton energy and adiabatic IPs) upon multiphoton PI, which are indicated as narrow hatched bars in Fig. 4(a). We conclude that, while $(\text{CsOH})_n$ clusters are most likely produced in $\text{Cs}_n + (\text{H}_2\text{O})_m$ reactions, the observed cluster masses $\text{Cs}(\text{CsOH})_n^+$ are subsequently formed by fragmentation upon ionization. This reaction channel is schematically summarized in the top lines of Fig. 4(b) for the example $n = 2$.

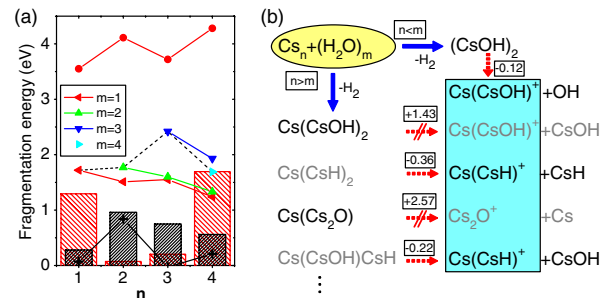


FIG. 4 (color online). (a) Fragmentation energies for the endothermic ejection of OH by $(\text{CsOH})_n$ (circles) and by $(\text{CsOH})_n^+$ (crosses), in comparison with surplus energy after multiphoton PI in eV (narrow bars). Triangles represent fragmentation energies of the reaction $\text{Cs}(\text{CsOH})_n^+ \rightarrow \text{Cs}(\text{CsOH})_{n-m}^+ + (\text{CsOH})_m$ vs surplus energy after PI (wide bars). (b) Schematic of reaction channels connecting reactants $\text{Cs}_n + (\text{H}_2\text{O})_m$ prepared in He nanodroplets (oval frame) with detected compounds containing 2 Cs atoms as an example (rectangular frame). Solid and dashed arrows depict chemical reactions and PI followed by fragmentation, respectively.

Besides the full oxidative hydrolysis reaction, incomplete reactions may occur in those He clusters in which a surplus of water with respect to Cs is not provided. This leads to the formation of compounds of the type $Cs_n(CsOH)_m$, where $n > 1$, and of $Cs_{n-1}(CsH)_m$, $Cs_{n-2}(Cs_2O)_m$, $Cs(CsOH)CsH$, and others. These compounds stem from intermediates of the reaction which are stabilized by the dissipative He droplet environment. Note that NaH formation was identified as the rate-determining step with a reaction barrier of 0.6 eV in the $Na_n + (H_2O)_m$ reaction [13]. The corresponding reaction and fragmentation channels are represented in the bottom lines of Fig. 4(b) for the particular case $n = 3$. Thus, there are 2 reaction channels that feed into the masses $Cs(CsOH)_n^+$, which explains the detected high abundances.

The stability of these compounds is theoretically analyzed with respect to the most probable fragmentation channel, the loss of $(CsOH)_m$. Figure 4(a) (triangles) depicts the fragmentation energies ΔE in comparison with surplus energies delivered by multiphoton PI (wide hatched bars). Interestingly, particularly high stability is obtained for $n = 3$; i.e., ΔE is high with respect to all 3 possible fragmentation channels. The same holds for neutral $Cs(CsOH)_n$. This is due to the regular geometric structure of $Cs(CsOH)_3^{0/+}$, which matches the cuboid rock-salt lattice with one unoccupied site, in which an electron is localized in the case of neutral $Cs(CsOH)_3$ [see the inset in Fig. 2(a)]. In particular, ΔE by far exceeds the excess energy deposited in the cluster upon two-photon PI. The same is true for $n = 1, 2$. The enhanced stability for $n = 3$ and the expected fragmentation of $Cs(CsOH)_4^+$ and higher masses into $Cs(CsOH)_3^+$ nicely explain the extraordinarily high abundance of that compound observed by PI (Fig. 2).

The mass spectra of progressions of the type $Cs_n(CsOH)_m^+$, $Cs_n(CsH)^+$, $Cs_n(Cs_2O)_m^+$, and $Cs_n(CsOH)_m(CsH)^+$, which show alternating abundances, are rationalized using the following simple picture. High stability is determined by the number n of valence electrons of the Cs_n part, which either form chemical bonds or pair up in even numbers. For example, $Cs(CsH)^+$ [$Cs(Cs_2O)^+$] are particularly stable, since one [two] electrons are needed for Cs binding to H [O], and the remaining electron is ejected upon ionization. This picture, which applies here due to predominantly ionic bonding of these small compound clusters, is confirmed by our theoretical results in terms of cluster stabilities with respect to fragmentation at a given PI energy. Differences between ΔE and surplus energy due to nonresonant PI, which determine whether photofragmentation is energetically allowed, are included in Fig. 4(b) for reaction products containing 3 Cs atoms. Hence, photofragmentation of $Cs(CsOH)_2$ and of $Cs(Cs_2O)$ is forbidden, and a high signal intensity is detected at masses of $Cs(CsOH)_2^+$ and $Cs(Cs_2O)^+$. In contrast, both $Cs(CsH)_2$ and $Cs(CsOH)CsH$ readily fragment into $Cs(CsH)^+$, which leads to high $Cs(CsH)^+$ signals at

the expense of the parent masses. The nice agreement of our model calculations, including both full as well as incomplete reactions, with experimental data supports our interpretation that reactions occur among the neutral low-spin alkali-metal clusters and water clusters prior to PI.

In conclusion, we find that, while Na and H_2O clusters in He droplets predominantly form van der Waals complexes, Cs_n clusters completely chemically react with $(H_2O)_m$ to form a variety of compounds despite the ultracold droplet environment. All prominent features are interpreted in terms of stabilities of individual compound clusters with respect to photofragmentation, as obtained from high-level molecular structure calculations. These experiments demonstrate the potential of He nanodroplets to serve as nanoscopic cryoreactors for probing elementary reactions at ultralow temperatures.

Stimulating discussions with U. Buck and C. P. Schulz are gratefully acknowledged. This work has been supported by the Deutsche Forschungsgemeinschaft.

*mudrich@physik.uni-freiburg.de

- [1] R. V. Krems, *Int. Rev. Phys. Chem.* **24**, 99 (2005).
- [2] E. R. Hudson *et al.*, *Phys. Rev. A* **73**, 063404 (2006).
- [3] J. P. Toennies, *Phys. Scr.* **76**, C15 (2007).
- [4] S. Willitsch *et al.*, *Phys. Rev. Lett.* **100**, 043203 (2008).
- [5] J. J. Gilijamse *et al.*, *Science* **313**, 1617 (2006).
- [6] J. P. Toennies and A. F. Vilesov, *Angew. Chem., Int. Ed.* **43**, 2622 (2004).
- [7] E. Lugovoj, J. P. Toennies, and A. Vilesov, *J. Chem. Phys.* **112**, 8217 (2000).
- [8] J. M. Merritt, S. Rudlas, and R. E. Miller, *J. Chem. Phys.* **124**, 084301 (2006).
- [9] M. Farnik and J. P. Toennies, *J. Chem. Phys.* **122**, 014307 (2005).
- [10] I. Hertel, C. Hüglin, C. Nitsch, and C. Schulz, *Phys. Rev. Lett.* **67**, 1767 (1991).
- [11] L. Bewig *et al.*, *J. Phys. Chem. A* **102**, 1124 (1998).
- [12] U. Buck and C. Steinbach, *J. Phys. Chem. A* **102**, 7333 (1998).
- [13] C. J. Mundy, J. Hutter, and M. Parrinello, *J. Am. Chem. Soc.* **122**, 4837 (2000).
- [14] C. Bobbert and C. Schulz, *Eur. Phys. J. D* **16**, 95 (2001).
- [15] C. Steinbach and U. Buck, *Phys. Chem. Chem. Phys.* **7**, 986 (2005).
- [16] P. Claas *et al.*, *J. Phys. B* **39**, S1151 (2006).
- [17] G. E. Douberly and R. Miller, *J. Phys. Chem. A* **111**, 7292 (2007).
- [18] C. P. Schulz *et al.*, *Phys. Rev. Lett.* **92**, 013401 (2004).
- [19] O. Bünermann and F. Stienkemeier (unpublished).
- [20] G. Niedner-Schatteburg and V. E. Bondybey, *Chem. Rev.* **100**, 4059 (2000).
- [21] Trucks *et al.*, GAUSSIAN 03 (revision B. 04), 2003.
- [22] J. P. Perdew, K. Burke, and M. Ernzerhof, *Phys. Rev. Lett.* **77**, 3865 (1996).
- [23] I. S. Lim *et al.*, *J. Chem. Phys.* **122**, 104103 (2005).